Proceedings of ALGORITMY 2012
pp. 161–171

ON SOME MODEL REDUCTION APPROACHES FOR SIMULATIONS OF PROCESSES IN LI-ION BATTERY*

OLEG ILIEV†, ARNULF LATZ‡, JOCHEN ZAUSCH§, AND SHIQUAN ZHANG¶

Abstract. In this work, some model reduction approaches for performing simulations with a pseudo-2D model of Li-ion battery are presented. A full pseudo-2D model of processes in Li-ion batteries is presented following [1], and three methods to reduce the order of the full model are considered. These are: i) directly reduce the model order using proper orthogonal decomposition, ii) using fractional time step discretization in order to solve the equations in decoupled way, and iii) reformulation approaches for the diffusion in the solid phase. Combinations of above methods are also considered. Results from numerical simulations are presented, and the efficiency and the accuracy of the model reduction approaches are discussed.

Key words. Pseudo-2D model, li-ion battery, model order reduction, proper orthogonal decomposition, fractional time step, model reformulation

AMS subject classifications. 65M08, 65M22, 65Z05

1. Introduction. Secondary Li-ion batteries used for technical applications are based on porous insertion electrodes. In most of the technical applications the porous electrodes are random structures of active particles bound together by a mixture of polymeric binder and soot for enhancing the electrical conductivity of the electrode. During charging Li-ions are de-intercalated from the anode particles into the electrolyte and transported through the electrolyte to the porous cathode. There they are intercalated at the surface of the cathode particles and then transported via diffusion into the interior of particles. It is well understood that the microstructure (e.g. size and arrangement of the active particles in the porous electrodes) significantly influence the performance of the battery. Going beyond porous structures, it has even been shown that specifically designed electrodes, can achieve a much larger power density [2], but still a lot of research is needed in order to quantitatively evaluate the influence of 3D structures. Available 3D microscale models include mass transport in the electrolyte and in the solid particles, coupled with an equation for the potential [3, 4] and more generally also with an additional equation for the temperature [5]. Solving these models is only possible on cuts through the whole cell covering nevertheless the whole cathode anode direction [6, 7]. Simulations on the complete microstructure is not yet possible due to the tremendous CPU demand. One approach to overcome this problem at least for random porous electrodes pioneered by the group of J. Newman [8] is to model the electrodes as effective random one

*This work was supported by Fraunhofer systems research electromobility FSEM (13N10599) and Young scholar's foundation of Sichuan University (2010SCU11076).

†Fraunhofer ITWM, Fraunhofer Platz 1, D-67663 Kaiserslautern, Germany. Technical University of Kaiserslautern, Kaiserslautern, Germany. Inst. of Mathematics, Bulgarian Academy of Science, Sofia, Bulgaria.(oleg.iliev@itwm.fraunhofer.de).

‡Fraunhofer ITWM, Fraunhofer Platz 1, D-67663 Kaiserslautern, Germany. (arnulf.latz@fraunhofer.itwm.fhg.de).

§Fraunhofer ITWM, Fraunhofer Platz 1, D-67663 Kaiserslautern, Germany. (jochen.zausch@fraunhofer.itwm.fhg.de).

¶Fraunhofer ITWM, Fraunhofer Platz 1, D-67663 Kaiserslautern, Germany. School of Mathematics, Sichuan University, Chengdu 610064, China. (shiquanz3@gmail.com).

dimensional porous media characterized by a porosity [9, 10, 11, 12, 13, 14, 15]. Their effective transport properties are obtained by averaging the properties of electrolyte and the active particles. In addition the transport within the particles is modeled as diffusive transport in one effective particle per volume element coupled to the transport in the effective porous medium. The separator is also described as effective porous medium. Thus a pseudo-2D model (i.e. 1D+1D model) for the full battery cell is obtained. Three dimensional extensions (more exact 3D+1D models), which allow to simulate complex shaped electrodes are possible [16]. These macroscopic models are solved by some numerical method, e.g., finite difference, finite volume or finite elements. One (representative) spherical particle is located in each grid node (for FDM and FVM), or in each quadrature point (for FEM), and the macroscopic model is coupled to the model in the particle (see the text below for details). The solution of the coupled model (called also *full model* below in the text) requires solving diffusion equation for each particle in an extra pseudo-dimension, namely in the radius r. Consequently, the number of unknown variables in this 1D+1D model is large, thus still requiring significant computational time. To obtain models which can be solved in real time further approaches for reducing the demanded computational times have appeared in the literature. The goal of this paper is to present a computational study of the performance of three model reduction approaches, when applied to simulation of processes in Li-ion battery.

First, consider the approach which was earlier presented in [1]. It exploits reduced order method, ROM, which is based on proper orthogonal decomposition, POD. The Authors claimed that this method is efficient for the pseudo-2D model, and they provided some simulation results for test cases. However, the parameters (and thus regimes) for simulation of real processes sometimes differ from conditions considered in test cases, and therefore more studies are required for the case of real parameters.

Further on, reformulation methods were used to avoid solving the diffusion equation in the active particles, see, e.g. [8, 3, 17, 18, 19, 20, 21]. These methods are based on approximating the concentration in solid phase by some selected functions of r, followed by volume averaging. The basis functions are global (defined from 0 to R), but very few of them are used. The aim of the volume averaging is to avoid solving the diffusion equation in the active particles. Zhang and White [20] compared some of the reformulation methods and discussed their efficiency in solving test examples.

In this paper, we consider both of the above methods and apply them in order to reduce the model order of the pseudo-2D li-ion battery model. In the case of ROM based on POD, we select a basic set of parameters and perform full simulations. After that the solution is used to form so called transform basis. The latter are used to form reduced order model, and later on to simulate the processes for other sets of parameters. We also review most of the reformulation methods and consider combination of reformulation and ROM-POD approaches. Further on, we consider one new way to reduce the the complexity of the problem, namely a fractional time step discretization, allowing to solve for all the unknowns in a decoupled way. The dominated part of the unknowns can be solved in parallel, and the other part can be combined with ROM-POD to further increase the efficiency.

The rest of the paper is organized as follows. In section 2 we describe the full model and the discretization. In section 3, we discuss the method of ROM based on POD and apply it to reduce the order of the full pseudo-2D model. In section 4, we present the fractional time step discretization and solve the full model in a decoupled way. In section 5, we review the reformulation methods and combine them with ROM.

TABLE 2.1
Governing equations and expressions

variable	equation		boundary conditions
c_s	$\frac{\partial c_s}{\partial t} = D_s \frac{1}{r^2}\frac{\partial}{\partial r}(r^2 \frac{\partial c_s}{\partial r})$		$-\frac{\partial c_s}{\partial r}\mid_{r=0} = 0,\ -\frac{\partial c_s}{\partial r}\mid_{r=R_{s,i}} = j_i$
c_e	$\epsilon_i \frac{\partial c_e}{\partial t} = D_{eff,i}\frac{\partial^2 c_e}{\partial x^2} + (1-t_+)a_i F j_i$		$-D_{eff,i}\frac{\partial c_e}{\partial x} = 0$
Φ_1	$\sigma_{eff,i}\frac{\partial^2 \Phi_1}{\partial x^2} = a_i F j_i$		$-\sigma_{eff,p}\frac{\partial \Phi_1}{\partial x} = I,\ \Phi_1\mid_{x=L_p+L_s+L_n} = 0$
Φ_2	$-\frac{\partial}{\partial x}(\kappa_{eff}\frac{\partial \Phi_2}{\partial x}) + \beta\frac{\partial}{\partial x}(\kappa_{eff}\frac{\partial ln c_e}{\partial x}) = a_i F j_i$		$-\kappa_{eff,i}\frac{\partial \Phi_2}{\partial x} = 0$
initial conditions	$c_{s,i}(r,0) = c_{s,i,0}$		$c_e(x,0) = c_0$
interface conditions			
$x = L_p$	$-D_{eff,p}\frac{\partial c_e}{\partial x} = -D_{eff,s}\frac{\partial c_e}{\partial x}$	$-\sigma_{eff,p}\frac{\partial \Phi_1}{\partial x} = 0$	$-\kappa_{eff,p}\frac{\partial \Phi_2}{\partial x} = -\kappa_{eff,s}\frac{\partial \Phi_2}{\partial x}$
$x = L_p + L_s$	$-D_{eff,s}\frac{\partial c_e}{\partial x} = -D_{eff,n}\frac{\partial c_e}{\partial x}$	$-\sigma_{eff,n}\frac{\partial \Phi_1}{\partial x} = 0$	$-\kappa_{eff,s}\frac{\partial \Phi_2}{\partial x} = -\kappa_{eff,n}\frac{\partial \Phi_2}{\partial x}$
expressions			

$$U_p = 4.199 + 0.0566tanh(-14.555\theta_p + 8.609) - 0.0275[(0.998-\theta_p)^{-0.492} - 1.901] - 0.157exp(-0.0474\theta_p^8) + 0.81exp[-40(\theta_p - 0.134)]$$

$$U_n = -0.16 + 1.32exp(-3.0\theta_n) + 10.0exp(-2000.0\theta_n))$$

$$\theta_p = c_{s,p,surf}/c_{s,p,max},\ \theta_n = c_{s,n,surf}/c_{s,n,max}$$

$$j_i = 2k_m(c_{s,i,max} - c_{s,i,surf})^{0.5}c_{s,i,surf}^{0.5}c_e^{0.5}sinh(\frac{0.5F}{RT}(\Phi_1 - \Phi_2 - U_i))$$

$$\sigma_{eff,i} = \sigma_i(1-\epsilon_i-\epsilon_{f,i}),\ a_i = \frac{3}{R_{s,i}}(1-\epsilon_i-\epsilon_{f,i}),\ \text{i=p,n}$$

$$\kappa_{eff,i} = (4.1253\times10^{-2} + 5.007\times10^{-4}c - 4.7212\times10^{-7}c^2 + 1.5094\times10^{-10}c^3 - 1.6018\times10^{-14}c^4)\epsilon_i^{brugg_i}$$

$$D_{eff,i} = D_e\epsilon_i^{brugg_i},\ i = p,s,n$$

Conclusions are given in section 6.

2. Full pseudo 2D model. The sketch of a LiMnO2-carbon battery is shown in Fig. 2.1. From left to right, the components of the battery are aluminum current collector, LiMnO2 positive electrode, separator, carbon negative electrode, and copper current collector. The governing equations and related expressions are summarized in Table 2.1 (see also [1]), and the parameters are given in Table 2.2.

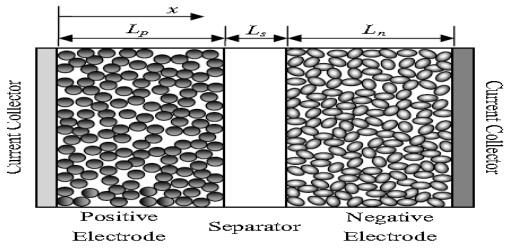

FIG. 2.1. *Schematic of a lithium battery*

For the discretization of the above model, cell centered finite volume method is adopted. The domain $(0, L_p + L_s + L_n)$ is divided into $N_p + N_s + N_n$ cells. Active particles are placed at the centers of those cells, which belong to the electrodes. The processes in the porous electrodes, described by macroscopic equations, are coupled via Butler-Volmer flux conditions on the surface of the particle to the processes in the particles, described by 1D model in spherical coordinates. Thus the pseudo-2D model assumes that the particles in the center of the grid cells (see Fig. 2.2) are typical and represent all other particles in the cell. The active solid particles are considered to have spherical form, and it is further assumed that processes in r direction dominate, so that 1D model can be used in each particle. The radius r of each particle is divided into N_r control volumes (cells). $N_r = 50$ is used in simulations presented here. The (macroscopic) $x-$ regions of the positive electrode, of the separator, and of

TABLE 2.2
Parameters

Parameter	Value	Unit	Parameter	Value	Unit
L_p	183	μm	$c_{s,p,max}$	22860	mol/m^3
L_s	52	μm	$c_{s,n,max}$	26390	mol/m^3
L_n	100	μm	$c_{s,p,0}$	3900	mol/m^3
$R_{s,p}$	8	μm	$c_{s,n,0}$	14870	mol/m^3
$R_{s,n}$	12.5	μm	σ_p	3.8	S/m
$D_{s,p}$	1.0×10^{-13}	m^2/s	σ_n	100	S/m
$D_{s,n}$	3.9×10^{-14}	m^2/s	$Brugg_p$	1.5	–
D_e	7.5×10^{-11}	m^2/s	$Brugg_s$	1.5	–
ϵ_p	0.444	–	$Brugg_n$	1.5	–
ϵ_s	1.0	–	k_p	2.334×10^{-11}	$mol/m^2s/(mol/m^3)^{1.5}$
ϵ_n	0.357	–	k_n	2.334×10^{-11}	$mol/m^2s/(mol/m^3)^{1.5}$
$\epsilon_{f,p}$	0.259	–	t_+	0.363	–
$\epsilon_{f,n}$	0.172	–	I	17.5(1C rate)	A/m^2
c_0	2000	mol/m^3	T	298	K

the negative electrode, are discretized into $N_p = 100$, $N_s = 70$, and $N_n = 100$ control volumes, respectively.

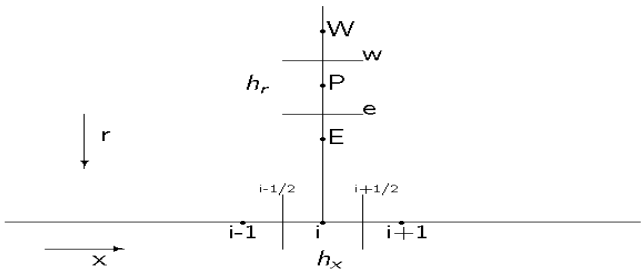

FIG. 2.2. *A typical volume in electrode*

Thus, with the selected Ns, at every grid node of the macroscopic grid (x- coordinate), there are 54 unknowns. They are arranged in the following order: the first 50 unknowns correspond to the concentration of lithium ions in the respective particle, numbered from the center to the surface of particle. The 51th unknown stands for the concentration on the surface of the particle, the 52th unknown stands for the concentration in the electrolyte, the 53th stands for the potential in the solid phase, and the last one stands for the potential in the electrolyte. The respective 54 equations arising after the discretization are numbered from i_1 to i_{54} and they look as follows:

$$
\begin{aligned}
\frac{dc_{s,P}}{dt} &= \frac{D_s}{r_P^2}\frac{r_e^2(c_{s,E}-c_{s,P})}{h_r^2} && (i_1)\\
\frac{dc_{s,P}}{dt} &= \frac{D_s}{r_P^2}\frac{r_e^2(c_{s,E}-c_{s,P})-r_w^2(c_{s,P}-c_{s,W})}{h_r^2} && (i_2)\cdots(i_{49})\\
\frac{dc_{s,P}}{dt} &= -\frac{r_e^2}{r_P^2 h_r}j-\frac{D_s}{r_P^2}\frac{r_w^2(c_{s,P}-c_{s,W})}{h_r^2} && (i_{50})\\
c_{s,surf} &= \frac{-3h_r j+9D_s c_{s,50}-D_s c_{s,49}}{8D_s} && (i_{51})\\
\epsilon\frac{dc_e}{dt} &= D_{eff}\frac{c_{e,i+1}-2c_{e,i}+c_{e,i-1}}{h_x^2}+(1-t_+)aj && (i_{52})\\
aFj &= \sigma_{eff}\frac{\Phi_{1,i+1}-2\Phi_{1,i}+\Phi_{1,i-1}}{h_x^2} && (i_{53})\\
aFj &= -\frac{\kappa_{eff,i+\frac12}(\Phi_{2,i+1}-\Phi_{2,i})-\kappa_{eff,i-\frac12}(\Phi_{2,i}-\Phi_{2,i-1})}{h_x^2}\\
&\quad+\frac{\kappa_{\beta_{i+\frac12}}(c_{e,i+1}-c_{e,i})-\kappa_{\beta_{i-\frac12}}(c_{e,i}-c_{e,i-1})}{h_x^2} && (i_{54})
\end{aligned}
\tag{2.1}
$$

Where $\kappa_\beta = \frac{\kappa_{eff}\beta}{c_e}$, $\kappa_{eff,i+\frac12}$ is harmonic average of $\kappa_{eff,i+1}$ and $\kappa_{eff,i}$, means $\kappa_{eff,i+\frac12} = \frac{2\kappa_{eff,i+1}\kappa_{eff,i}}{\kappa_{eff,i+1}+\kappa_{eff,i}}$, and similar to $\kappa_{eff,i-\frac12}$, $\kappa_{\beta_{eff,i+\frac12}}$ and $\kappa_{\beta_{eff,i-\frac12}}$.

Remark 2.1. In the above discretization, j equal to j_p in positive electrode, zero in separator and j_n in negative electrode. For the surface concentration, as there is no governing equation for it in Table 2.1, we just interpolate it with the two nearest unknowns inside the particle, combined with the surface condition. For the nodes in the separator, only equations with numbers (i_{52}) and (i_{54}) are used, all other unknowns are assigned to be zeros.

Remark 2.2. For the treatment of interface conditions at $x = L_p$ (similarly at $x = L_p + L_s$), we use $-D_{eff,p}\frac{\partial c_e}{\partial x} = -D_{eff,s}\frac{\partial c_e}{\partial x} = -D_{eff,ps}\frac{c_{e,s}-c_{e,p}}{0.5(h_p+h_s)}$ and $-\kappa_{eff,p}\frac{\partial \Phi_2}{\partial x} = -\kappa_{eff,s}\frac{\partial \Phi_2}{\partial x} = -\kappa_{eff,ps}\frac{\Phi_{2,s}-\Phi_{2,p}}{0.5(h_p+h_s)}$, where $D_{eff,ps}$ is harmonic average of $D_{eff,p}$ and $D_{eff,s}$, and similar to $\kappa_{eff,ps}$.

For the time discretization, first order backward Euler is adopted. Uniform time step is used, and standard Newton-Raphsion method is applied to solve the obtained nonlinear system.

3. Reduced order model based on POD.

3.1. Method description. Here we adopt the standard procedure for POD based model order reduction [1, 22]. The basic idea for model order reduction is that instead of solving the full model solution $\mathbf{x}$ directly, we first solve some reduced variable y, and obtain the desired solution by $\mathbf{x} = By$. Where the basis B is pre-constructed by using POD method for the full model solution of one base case and choose very few dominated eigenvectors, thus the reduced system for y is much smaller than the full model system for $\mathbf{x}$. More details about the method and algorithm can be found in ITWM report [23].

3.2. Results and discussion. To test the efficiency of the presented ROM method, we consider three different examples here. In all the examples, the results obtained with ROM are compared with the solution of the full model.

(1) We choose the base case to be 1C discharge with the parameters given in Table 2.2, and change initial conditions ($c_e(x,0) = 2500, c_{s,n}(r,0) = 18870$) as tested case. In this example, the base case and the tested case differ only in the values for the initial conditions. The full model solution and the ROM solution of the tested case are compared in Fig. 3.1. We can see that the ROM with only 27 eigenvectors (for comparison, the size of the full system is 14580) approximate the solution of the full model very well.

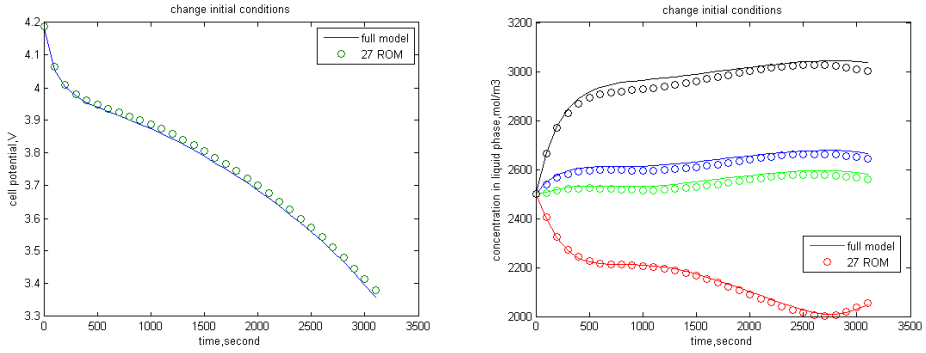

FIG. 3.1. *Change initial conditions* Left*: cell potential;* Right*: concentration at interfaces*

(2) we choose the same base case as in the first example, but choose as tested case a problem with characterized by 10C discharge. All other parameters are the same as in the base case. For this example, we can also obtain very accurate results with very few eigenvectors.

(3)The third considered example corresponds to simulation of discharge-charge cycles. In one cycle, the battery is first discharged at 1C rate until the cell potential decrease to 3.0 V., followed by a 1C charge process up to 4.3 V, and at the last stage of the cycle the battery is charged at 4.3 V until the current decreases to 10 mA. In the simulations, we choose the solution of one cycle as a base solution, form reduced system and use the latter to simulate many cycles. In this case, we can obtain similar results as example 1 and 2 by choosing few eigenvectors.

4. Fractional time step discretization.

4.1. Method description. Consider again the full model. When first order backward Euler is used for time discretization, the resulting discretized system at time t_{n+1} is written as follows

$$M\frac{\mathbf{x}^{n+1}-\mathbf{x}^n}{\triangle t} = f(\mathbf{x}^{n+1})$$

We divide all the unknowns into two classes, namely $\mathbf{x} = (\mathbf{x}_e, \mathbf{x}_p)$, where we choose $\mathbf{x}_p = (c_s, c_{s,surf})$ as concentration in the particles, and $\mathbf{x}_e = (c_e, \Phi_1, \Phi_2)$ to be collection of the remaining unknowns. With the new notations, the original full

model system can also be solved by the following decoupled way:

$$M_e \frac{\mathbf{x}_e^{n+\frac{1}{2}} - \mathbf{x}_e^n}{\triangle t} = f_1(\mathbf{x}_e^{n+\frac{1}{2}}, \mathbf{x}_p^n) \tag{4.1}$$

$$M_p \frac{\mathbf{x}_p^{n+1} - \mathbf{x}_p^n}{\triangle t} = f_2(\mathbf{x}_e^{n+\frac{1}{2}}, \mathbf{x}_p^{n+1}) \tag{4.2}$$

The above predictor-corrector discretization means that at each time step we first solve for $\mathbf{x}_e$ using the solution of $\mathbf{x}_p$ at the previous time, and after that solve for $\mathbf{x}_p$ at the new time step, using just computed $\mathbf{x}_e$. Note, the questions about the theoretical study on the stability of this fractional time step discretization are not studied here. We can just note that our simulations show that it is worth to use this approach.

Remark 4.1. Note that in this particular problem $\mathbf{x}_p$ contains much more unknowns compared to $\mathbf{x}_e$, and that one can solve the predictor step for each particle separately, as long as the values from the previous time step are used for $\mathbf{x}_e$. As a result, this decoupled solve works much faster than the coupled solve for the full model.

Remark 4.2. For the solve with respect to $\mathbf{x}_e$ at each time step, we can use the previous ROM method in order to reduce the order of this system. This combination of using decoupled solve (fractional time step discretization) and ROM, can further improve the efficiency.

4.2. Results and discussion. We test coupled and decoupled system in two cases: 1C discharge and 10C discharge. For decoupled system, we need some restrictions on the time step. If uniform time step is used, the time step need to satisfy $\triangle t < 70s$ for 1C case and $\triangle t < 7s$ for 10C case. If the time step satisfy these conditions, solving the decoupled system is much faster than solving the coupled system and, and the results obtained by the two approaches are very close. It should be noted that often very large time steps (even if allowed by the stability consideration) can not be used in the simulations, because this would lead to lose of accuracy. See Fig. 4.1 for the results of cell potential.

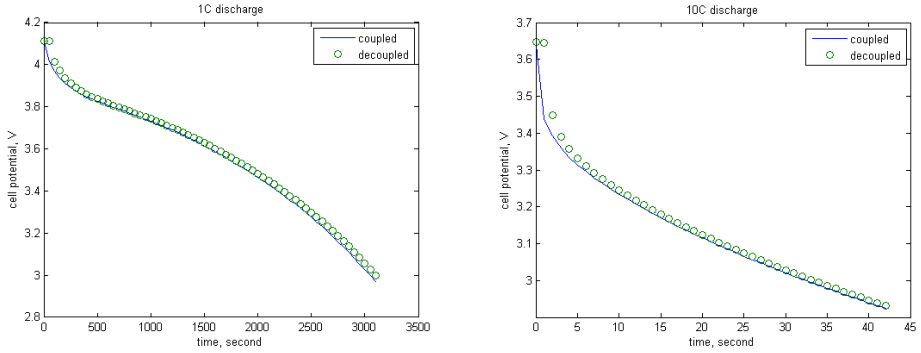

FIG. 4.1. *Cell potential.* Left*: 1C rate;* Right*: 10C rate.*

As pointed out in Remark 4.2, the above presented ROM approach presented can be used to solve for $\mathbf{x}_e$ at each time step. The results from such an approach for example 2 are given in Fig. 4.2. It can be seen that in this case the solution of the full model is approximated very well.

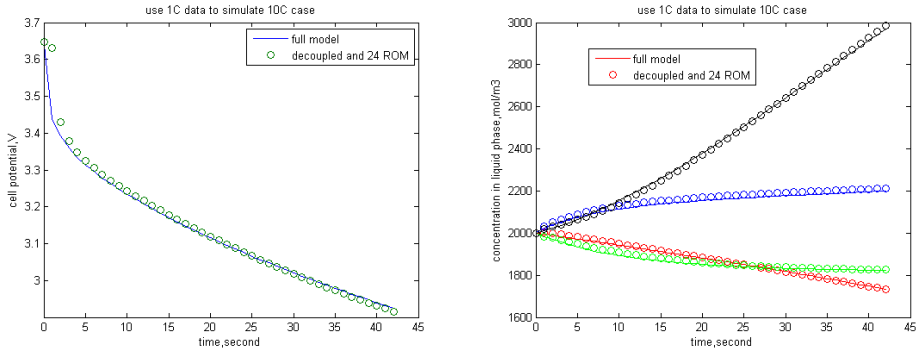

FIG. 4.2. *Change C rates* Left*: cell potential;* Right*: concentration at interfaces*

5. Reformulation of particle diffusion. In the full model, most of unknowns come from the discretization of the following diffusion equation inside the particle

$$\frac{\partial c}{\partial t} - D_s \frac{1}{r^2}\frac{\partial}{\partial r}(r^2 \frac{\partial c}{\partial r}) = 0 \tag{5.1}$$

with boundary condition

$$D_s \frac{\partial c}{\partial r} = 0 \quad at\ r = 0, \qquad D_s \frac{\partial c}{\partial r} = -j \quad at\ r = R_p \quad for\ t \geq 0$$

where j is the pore wall flux at the surface of particle and R_p is the radius of the particle. If we can avoid solving this equation, then the number of unknowns will decrease sharply. This is called Macro-Micro scale coupled simulation or reformulation of diffusion in solid phase. Below we will shortly review some of the existing methods in this area, will discuss their advantages and disadvantages, and will combine best of them with the above introduced ROM method.

Duhamel's superposition method [8] was the first approximation method used in the porous electrode model. It relates the solution of a boundary value problem with time dependent boundary conditions to the solution of a similar problem with time-independent boundary conditions by means of a simple relation.

By assuming the li-ion diffusion inside the particle is some polynomial and using the volume averaging technique, two kind of polynomial reformulation methods (called lower order (quadratic polynomial) and higher order (fourth order polynomial)) are proposed in [18]. Similarily, by assuming a parabolic concentration profile in the diffusion layer and using the volume average technique, [3] determined the diffusion length to be $l_s = R_p/5$ for spherical particles. Liu [19] applied pseudo steady state (PSS) method, which is a form of a finite integral transform technique to eliminate the independent spatial variable r from the solid phase diffusion equation.

It is reported in [20] that Duhamel's superposition method is more CPU time consuming than the full model, so we don't consider it here. PSS is numerically unstable as the values of the introduced there non-physical variables q_m are too large (10^{10} to 10^{50} for our test cases). Low order polynomial and diffusion length method are exactly the same in our cases, they work well for low current rate discharge but do not work for high discharge rate. High order polynomial can work with all the current rates, but the accuracy with higher discharge rate is not very good, see Fig. 5.1. So next we only describe the the correct diffusion length method and Galerkin

reformulation method in detail, the details for the review of other methods can be found in [20, 23].

5.1. Correct diffusion length method. Wang and Srinivasan [17] corrected the diffusion length method by empirically incorporating an intuitively expressed time dependent term into the diffusion length equations:

$$\frac{d}{dt}\overline{c}(t) + 3\frac{j}{R_p} = 0 \tag{5.2}$$

$$\frac{D_s}{l_s}[c_s(t) - \overline{c}(t)] = -j(1 - exp(-\frac{4}{3}\frac{\sqrt{D_s t}}{l_s})) \tag{5.3}$$

In this way, at each grid cell in electrodes, we only need to solve the above equations for $\overline{c}(t) = \int_{r=0}^{R_p} 3r^2 c(r,t)dr$ and $c_s(t) = c(R_p, t)$, and avoid solving (5.1).

5.2. Galerkin reformulation. Galerkin reformulation [21] is a modification of PSS method. By assuming $c(r,t) = a(t) + b(t)(r^2) + \sum_{m=1}^{N_q} \frac{d_m(t)sin(\lambda_m r)}{r}$ and similar volume average technique, the reformulation is:

$$\frac{d}{dt}\overline{c}(t) + 3\frac{j}{R_p} = 0 \tag{5.4}$$

$$\frac{D_s}{R_p}[c_s(t) - \overline{c}(t)] = -\frac{j}{5} + 2j\sum_{m=1}^{N_q}\frac{1}{\lambda_m^2} - \frac{D_s}{R_p}\sum_{m=1}^{N_q}\lambda_m^2 sin(\lambda_m)Q_m \tag{5.5}$$

$$\frac{dQ_m}{dt} + \frac{D_s}{R_p^2}\lambda_m^2 Q_m - \frac{2}{R_p\lambda_m^2 sin(\lambda_m)}j = 0, \quad m = 1\cdots N_q \tag{5.6}$$

$$\lambda_m = tan(\lambda_m) \quad m = 1\cdots N_q \tag{5.7}$$

5.3. Results and discussion. For the test case here, the correct diffusion length method and Galerkin reformulation with $N_q = 4$ work well for all the discharge rates, see Fig. 5.1 for the case of 10C discharge.

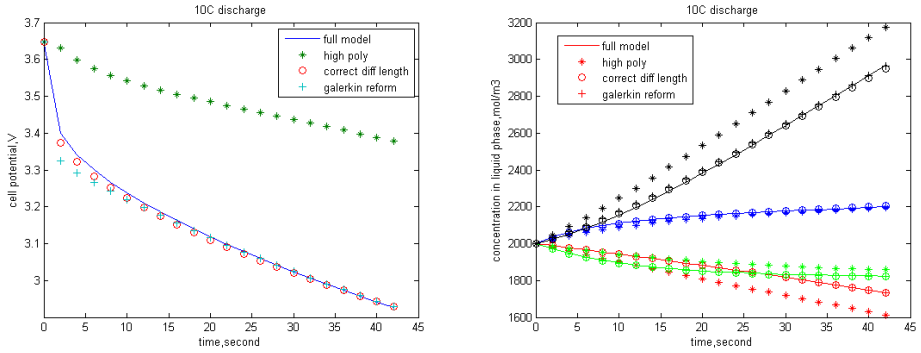

FIG. 5.1. *10C discharge.* Left*: cell potential;* Right*: concentration.*

The reformulated system for the particle can be combined with the above introduced ROM method to further reduce the system order. The results obtained with a combined use of ROM and the correct diffusion length method are given in Fig. 5.2 for the case of change different initial conditions.

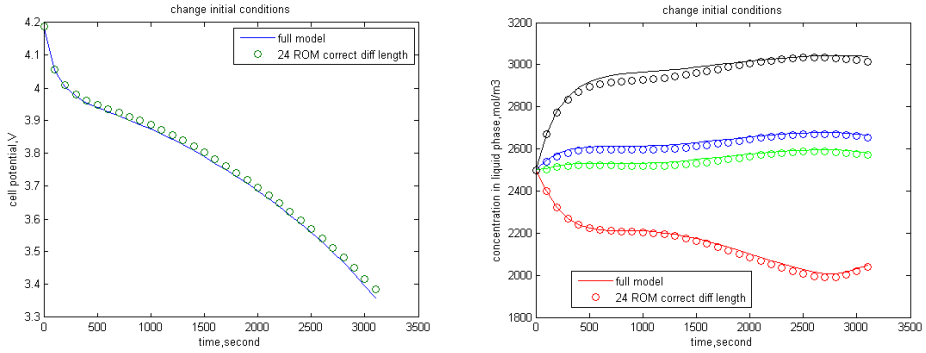

FIG. 5.2. *Change initial conditions* Left*: cell potential;* Right*: concentration at interfaces*

6. Conclusion. The main goal of this paper is to discuss various model reduction approaches for simulations of Li-ion transport described by pseudo-2D model of the battery. For ROM based on POD, provided the solution for a basic case (i.e., for a basic set of parameters) is known, we can decompose this solution via POD, choose the dominating eigenvectors to form a reduced order model, ROM, and further use this ROM to compute approximate solutions of the pseudo 2D model for other sets of parameters. Furthermore, it was stated that a decoupled solve, with some minor restriction on time step, is much faster than a coupled solve for the full model, while preserving good accuracy. Finally, several approaches for the reformulation of diffusion in solid phase were discussed, and it was shown that the correct diffusion length method and Galerkin reformulation work well for the test cases considered here. We also show that both, the decoupled solve and the diffusion reformulation method, can be combined with ROM based on POD in order to further increase the computational efficiency.

REFERENCES

[1] L. CAI, R. E. WHITE, *Reduction of model order based on proper orthogonal decomposition for lithium-ion battery simulations*, J. Electrochem. Soc., 156(2009), pp. A154–A161.

[2] H. ZHANG, X. YU AND P. V. BRAUN, *Three-dimensional bicontinuous ultrafast-charge and -discharge bulk battery electrodes*, Nature Nanotechnology, 6(2011), pp. 277–281.

[3] C. Y. WANG, W. B. GU, B. Y. LIAW, *Micro-macroscopic coupled modeling of batteries and fuel cells I. model development*, J. Electrochem. Soc., 145(1998), pp. 3407–3417.

[4] A. LATZ, J. ZAUSCH AND O. ILIEV, *Modeling of species and charge transport in Li–Ion Batteries based on Non-equilibrium Thermodynamics*, Lecture Notes in Computer Science, 6046(2011), pp. 329–337.

[5] A. LATZ AND J. ZAUSCH, *Thermodynamic consistent transport theory of Li-ion batteries*, Journal of Power Sources 196(2011), pp. 3296–3302.

[6] C. W. WANG AND A. M. SASTRY, *Mesoscale Modeling of Li-Ion Polymer Cell*, J. Electrochem. Soc., 154(2007), pp. A1035–1047.

[7] G. B. LESS, J. H. SEO, S. HAN, A. M. SASTRY, J. ZAUSCH, A. LATZ, S. SCHMIDT, C. WIESER, D. KEHRWALD, AND S. FELL, *Micro-Scale Modeling of Li-ion Batteries: Parameterization and Validation*, preprint 2012.

[8] M. DOYLE, T. F. FULLER AND J. NEWMAN, *Modeling of galvanostatic charge and discharge of the lithium/polymer/insertion cell*, J. Electrochem. Soc., 140(1993), pp. 1526–1533.

[9] T. F. FULLER, M. DOYLE AND J. NEWMAN, *Simulation and optimization of the dual lithium ion insertion cell*, J. Electrochem. Soc., 141(1994), pp. 1–10.

[10] G. G. BOTTE, V. R. SUBRAMANIAN, R. E. WHITE, *Mathematical modeling of secondary lithium batteries*, Electrochimica Acta, 45(2000), pp. 2595–2609.

[11] W. B. Gu and C. Y. Wang, *Thermal-electrochemical modelling of battery systems*, J. Electrochem. Soc., 147(2000), pp. 2910–2922.
[12] L. Song and J. W. Evans, *Electrochemical-thermal model of lithium polymer batteries*, J. Electrochem. Soc., 147(2000), pp. 2086–2095.
[13] M. Doyle and Y. Fuentes, *Computer simulations of a lithium-ion polymer battery and implications for higher capacity next-generation battery designs*, J. Electrochem. Soc., 150(2003), pp. A706–A713.
[14] V. Srinivasan and C. Y. Wang, *Analysis of electrochemical and thermal behavior of li-ion cells*, J. Electrochem. Soc., 150(2003), pp. A98–A106.
[15] G. Sikha, B. N. Popov and R. E. White, *Effect of porosity on the capacity fade of a lithium-ion battery*, J. Electrochem. Soc., 151(2004), pp. A1104–A1114.
[16] J. Zausch and A. Latz, *Derivation and Simulation of a full 3D porous electrode model of Li Ion batteries*, to be published, 2012.
[17] C. Y. Wang and V. Srinivasan, *Computational battery dynamics (CBD) electrochemical/thermal coupled modeling and multi-scale modeling*, J. Power Sources, 110(2002), pp. 364–376.
[18] V. R. Subramanian, V. D. Diwakar and D. Tapriyal, *Efficient macro-micro scale coupled modeling of batteries*, J. Electrochem. Soc., 152(2005), pp. A2002–A2008.
[19] S. Liu, *An analytical solution to Li/Li^+ insertion into a porous electrode*, Solid State Ionics, 177(2006), pp. 53–58.
[20] Q. Zhang and R. E. White, *Comparison of approximate solution methods for the solid phase diffusion equation in a porous electrode model*, J. Power Sources, 165(2007), pp. 880-886.
[21] V. Ramadesigan, V. Boovaragavan, J. C. Pirkle and V. R. Subramanian, *Efficient reformulation of solid-phase diffusion in physics-based lithium-ion battery models*, J. Electrochem. Soc., 157(2010), pp. A854–A860.
[22] K. Kunisch and S. Volkwein, *Control of the Burgers Equation by a Reduced-Order Approach Using Proper Orthogonal Decomposition*, J. Optimization Theorey and Applications, 102(1999), pp. 345–371.
[23] O. Iliev, A. Latz, J. Zausch and S. Zhang, *An overview on the usage of some model reduction approches for simulations of Li-ion transport in batteries*, Fraunhofer ITWM report (214), 2012.